

Optical conductivity of the Hubbard model at finite temperature

José A. Riera

*Center for Computationally Intensive Physics,
Physics Division, Oak Ridge National Laboratory, Oak Ridge, Tennessee 37831
and Department of Physics and Astronomy, Vanderbilt University, Nashville, Tennessee 37235*

Elbio Dagotto

*Department of Physics, National High Magnetic Field Laboratory, Florida State University, Tallahassee, Florida 32306
(Received 26 January 1994)*

The optical conductivity, $\sigma(\omega)$, of the two-dimensional one-band Hubbard model is calculated at finite temperature using exact diagonalization techniques on finite clusters. The in-plane dc resistivity, ρ_{ab} , is also evaluated. We find that at large U/t and temperature T , ρ_{ab} is approximately linear with temperature. We also observed that $\sigma(\omega)$ displays charge excitations, a midinfrared (MIR) band, and a Drude peak. The combination of the Drude peak and the MIR oscillator strengths leads to a conductivity that decays slower than $1/\omega^2$ at energies smaller than the insulator gap near half filling.

Experimentally, it has been observed that the in-plane dc resistivity ρ_{ab} of the hole-doped high-temperature superconductors is linear with temperature when the hole-doping fraction is optimal, i.e., when the critical temperature (T_c) is maximum.¹ This simple phenomenological law is still one of the most puzzling features of the normal state of the cuprates. A possible explanation of this behavior using the Bloch-Grüneisen formula (which is based on electron-phonon scattering) seems unlikely,² and thus mechanisms based on scattering by spin fluctuations have been proposed. The ac conductivity, $\sigma(\omega)$, also presents interesting features. A midinfrared band (MIR) has been observed inside the charge-transfer gap of the insulating parent compound.³ In addition, at small frequency (relative to the gap) $\sigma(\omega)$ decays as $1/\omega$, instead of the more standard Drude behavior $1/\omega^2$. This effect can be phenomenologically described by an energy-dependent lifetime $\tau(\omega) \sim \omega^{-1}$. Several theoretical mechanisms have been proposed to explain these features. Most are based on simple mean-field solutions of electronic Hubbard or t - J -like models, but the validity of these approximate descriptions is unclear. An alternative approach involves direct numerical analysis of these models.⁴ Recently, there has been considerable progress in this approach and several studies of $\sigma(\omega)$ on finite clusters using exact diagonalization techniques (at zero temperature) have been reported and compared to analytical approaches.^{5,6} The presence of the MIR band has been explained as due to the considerable spectral weight located in the incoherent part of the hole spectral function, and the anomalous $1/\omega$ decay was attributed to a combination of oscillator strength between the MIR band and the zero frequency Drude peak at zero frequency in the metallic regime.⁴

In this paper we report a numerical study of the two-dimensional (2D) one-band Hubbard model at finite temperature using the exact diagonalization approach on small clusters. Little work has been carried out previously at nonzero temperature using this technique, since

the full set of eigenvalues and eigenvectors of the finite cluster is needed to determine thermal properties. This substantially increases the memory and CPU requirements relative to zero-temperature properties.⁷ Here we evaluate both $\sigma(\omega)$ and ρ_{ab} and attempt a rough comparison of our results with experiments. The calculation of transport properties of a weakly dissipative system in the context of many-body problems generally follows the Kubo formulation, which relates the conductivity to a current-current correlation function. This approach has been widely used in the context of Hubbard-like models to describe strongly correlated systems. The real part of the conductivity at finite temperature is given by

$$\sigma(\omega) = \pi \frac{(1 - e^{-\beta\omega})}{\omega Z} \sum_{n,m} e^{-\beta E_n} |\langle n | j_x | m \rangle|^2 \times \delta(\omega + E_n - E_m), \quad (1)$$

where $|n\rangle$ is an eigenstate of the Hubbard Hamiltonian with eigenvalue E_n , Z is the partition function, β the inverse of the temperature, and j_x the current operator in the x direction. The rest of the notation is standard, and details can be found in textbooks.⁸

The diagonalization of the Hubbard model was carried out on small square clusters. In each subspace corresponding to a given set of quantum numbers (momentum, z component of the total spin and parity under spin reversal) we computed all the eigenvalues and eigenvectors in two steps. First, the matrix was reduced to a tridiagonal form using the Householder algorithm. We then diagonalized the resulting matrix using a standard QL algorithm. Since in general we have to deal with complex hermitian matrices, we developed hermitian versions of the subroutines TRED2 and TQLI of the *Numerical Recipes* package.⁹ In principle, the total operation count for both subroutines scales as $\sim N_H^3$, where N_H is the dimension of the matrix to be diagonalized. However, since the innermost loops could be vectorized, we found

that the coefficient of the N_H^3 was four orders of magnitude smaller than the coefficient of N_H^2 term on a Cray YMP. The total CPU time required to diagonalize the largest matrix with $N_H = 540$ was approximately 23 sec on a Cray YMP supercomputer and the total memory required for the diagonalization of a $N_H \times N_H$ matrix was $2 \times N_H^2 + 4 \times N_H$ words. Both CPU time and memory requirements compare well with similar subroutines in other packages such as IMSL or NAG. The calculation of $\sigma(\omega)$ itself was considerably more CPU time consuming than the diagonalization procedure. According to Eq. (1), the total operation count in a subspace of dimension N_H and for a fixed temperature scales as N_H^4 . However, in the calculation of the matrix $\langle n|j_x|m \rangle$ one can take advantage of its sparse nature, thus effectively reducing the dependence from N_H^4 to N_H^3 . Moreover, a set of measurements at different temperatures could be done with almost the same CPU time as a single temperature by appropriately rearranging the loops and vectorizing the innermost one.

Although the technique applied here works equally well for the Hubbard and t - J models, we have concentrated only on the Hubbard model, which possesses excitations across the gap that are important for comparison of $\sigma(\omega)$ with experiments. These calculations were carried out on small square clusters of eight and ten sites, similar to those used previously in the study of the Heisenberg model and other systems.^{10,4} On finite systems it is important to choose the boundary conditions to appropriately minimize finite-size effects. In the present study we decided to use antiperiodic boundary conditions (APBC's).¹¹ In the eight-site cluster with APBC the noninteracting limit $U/t = 0$ has four levels with energy $-2t$, and another four levels with energy $+2t$. In the half-filled case, and with $U/t > 0$, two bands exist separated by a gap, which grows as U/t increases. This behavior is also expected for the Hubbard model in the bulk limit. When holes are introduced, they are energetically favored to appear in the lower band. In contrast, the same cluster with periodic boundary conditions (PBC's) contains six levels of zero energy at $U/t = 0$, one state with energy $-2t$ and another with energy $+2t$. The large zero-energy degeneracy appears to produce large finite-size artifacts in the PBC case at finite coupling, and for this reason APBC's will be used in this paper.

The application of Eq. (1) to Hubbard-like models involves some complications. One problem is that an isolated, finite system, such as the clusters analyzed in any computational study, cannot show resistive behavior. Thus, the resistivity of a metallic ground state at zero temperature must vanish, since a Drude-like weight $D\delta(\omega)$ appears at zero frequency in the conductivity. In fact, Eq. (1) implies that a δ function is always present at zero frequency if any eigenstate of the Hamiltonian satisfies $|\langle n|j_x|m \rangle| \neq 0$ with $E_n = E_m$. Therefore, electron-electron interactions (Umklapp processes) are not sufficient to produce dissipation, and the dc resistivity of the Hubbard model is zero at all temperatures.¹² On finite systems with twisted BC's the calculation of the Drude weight is carried out indirectly, using the two-dimensional sum rule

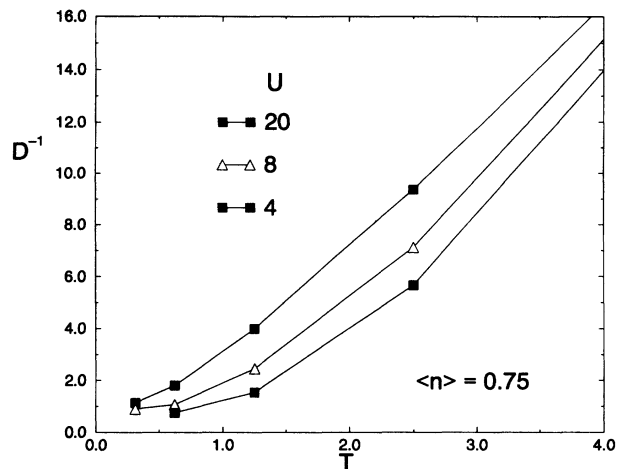


FIG. 1. The inverse of the Drude weight, D^{-1} , obtained numerically on an eight-site cluster with APBC, as a function of temperature (D and T in units of the hopping parameter t). The results are shown for couplings ranging from strong ($U/t = 20$) to weak coupling ($U/t = 4$). The filling fraction is shown in the figure.

$$\int_0^{\infty} d\omega \sigma(\omega) = \frac{\pi e^2}{4N} \langle -\hat{T} \rangle, \quad (2)$$

where $\langle \hat{T} \rangle$ is the thermal average of the kinetic energy operator. Assuming the existence of a contribution $D\delta(\omega)$ at zero energy, we obtain

$$\frac{D}{2\pi e^2} = \frac{\langle -\hat{T} \rangle}{4N} - \frac{1}{\pi e^2} \int_{0+}^{\infty} d\omega \sigma(\omega), \quad (3)$$

where both terms on the right-hand side (rhs) of Eq. (3) can be calculated numerically. Following this procedure, the inverse of the Drude weight D^{-1} is plotted in Fig. 1 as a function of temperature for several couplings U/t , and at a filling of six electrons on the eight-site cluster ($\langle n \rangle = 0.75$). D^{-1} is proportional to the dc resistivity, once a finite width is given to $\delta(\omega)$ to mimic dissipative processes not included in the Hamiltonian. It is interesting to note that for $T > t$ and strong coupling, D^{-1} is approximately linear with temperature. This is in agreement with the predictions of Rice and Zhang¹³ for the large U/t limit. On reducing the Hubbard coupling U/t , we find that D^{-1} acquires curvature in T , and in the weak coupling region $D^{-1} \sim T^2$. This behavior is consistent with the quadratic temperature dependence of the resistivity expected for a Fermi liquid. Now we will consider how our results can be compared with experiment,¹ at least at a qualitative level. First, note that for $t = 0.4$ eV a temperature of $1t$ corresponds to approximately 4600 K, which is much higher than the maximum experimental temperature for ρ_{ab} of ≈ 800 K and higher than the melting temperature of the cuprates. In principle we should reduce the temperature in our cluster calculations for this comparison. Unfortunately, at experimentally relevant temperatures the finite-size effects on the cluster are greatly increased, so that erratic behavior of the Drude weight as a function of $\langle n \rangle$ and U/t is observed. We estimate that for temperatures smaller than

$t/4 \approx 1200$ K our finite-cluster results are not representative of the bulk limit (this same limiting temperature of $t/4$ is suffered by quantum Monte Carlo techniques at finite hole density and by high-temperature expansion series. For details see Ref. 4). It is thus more convenient to extrapolate the experimental results to higher temperatures, since the slope $d\rho_{ab}/dT$ is accurately known experimentally. The physics leading to melting of the cuprates is unrelated to the electronic behavior in the CuO_2 planes we want to explore, and thus this assumption is reasonable. We believe that in the absence of the processes that lead to melting, ρ_{ab} would continue being linear even at temperatures as high as $t/4$.

The slopes $d\rho_{ab}/dT$ (at the optimal doping concentration) are very similar among the different cuprates, and range from $d\rho_{ab}/dT \approx 1 \mu\Omega \text{ cm} / \text{K}$ for $\text{Bi}_2\text{Sr}_2\text{CuO}_6$ (Bi2201) to $d\rho_{ab}/dT \approx 0.5 \mu\Omega \text{ cm} / \text{K}$ for $\text{YBa}_2\text{Cu}_3\text{O}_{7-\delta}$ (Y123) with a T_c of 90 K. The extrapolated experimental results are shown in Fig. 2 (dotted lines). The theoretical predictions obtained from the present cluster calculations are also shown in this figure (open squares and triangles), and were obtained by plotting D^{-1} times a parameter with units of $\mu\Omega \text{ cm}$, which sets the relative scale between our calculations and experiment. (Physically this parameter contains information about scattering processes not incorporated in the Hubbard model, so the overall normalization of our predictions is not determined and has been taken from experiment. To simplify the calculation we have assumed that this parameter is temperature independent.) Given this freedom to fix the overall normalization, a reasonable agreement is observed between theoretical predictions and extrapolated experimental results for ρ_{ab} over the range of temperatures for

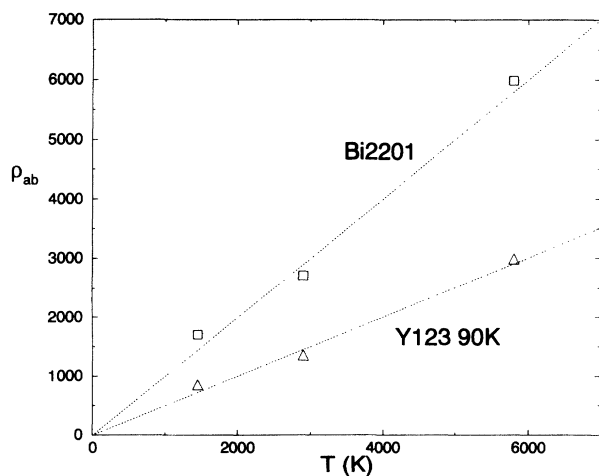


FIG. 2. The dc in-plane resistivity ρ_{ab} as a function of temperature. The dotted lines correspond to experimental results for Bi2201 and Y123, extrapolated to high temperatures comparable to the hopping parameter [t is taken to be 0.4 eV (≈ 4600 K)]. The squares and triangles are numerical results obtained on the eight-site cluster with APBC for $U/t = 20$ and filling fraction $\langle n \rangle = 0.75$. D^{-1} was multiplied by a constant with units of inverse time to set the scale. The value of this constant was chosen independently for the two compounds. ρ_{ab} in units of $\mu\Omega \text{ cm}$.

which we consider the cluster results reliable. This encouraging result suggests that the simple one-band Hubbard model may describe some normal-state properties of the cuprates. There is a slight upward curvature in the results, which is not surprising, since the experimentally measured ρ_{ab} is linear with temperature only at one particular density.¹⁴ The filling fraction we have used, $\langle n \rangle = 0.75$, may correspond to the slightly “overdoped” regime of the cuprates.¹⁵

Now let us analyze the ac conductivity. To allow a comparison with experiment we follow Imry¹⁶ and give each δ function of Eq. (1) a finite width, to account for scattering through other processes not included in the model, such as phonons and disorder. This width ϵ should be larger than the mean interlevel spacing in order to mimic a continuum of states. ϵ^{-1} can be considered to be a phenomenological relaxation time introduced to account for dissipative processes not included in the Hamiltonian (whose temperature dependence will be neglected in this first exploratory analysis). ϵ is a free parameter in our study (in addition to the electronic density $\langle n \rangle$ and the coupling U/t of the Hubbard model) and we adopt $\epsilon = 0.33$ for the following discussion. In Fig. 3, $\sigma(\omega)$ is shown for the eight-site cluster at several densities and couplings. The Drude peaks at zero frequency are incorporated in the plots. Figure 3(a) shows the result for a temperature comparable to the antiferromagnetic exchange coupling J ($T = 0.3125t$), and for illustration we use $U/t = 20$ to enlarge the gap in the results. At half filling (eight electrons), most of the spectral weight is located at $\omega > 5$ (in t units), in other words these are charge excitations, as expected. As the density $\langle n \rangle$ is decreased, spectral weight is transferred from the high-frequency charge excitations to lower frequencies. A Drude peak is formed, and considerable weight appears within the insulating gap. (This may be associated with the MIR band observed in the cuprates as has been discussed extensively in the literature.⁴) Figure 3(b) shows the same cluster at $T = 1.25t$ and coupling $U/t = 8$, which may be more representative of the cuprates.⁴ Qualitatively, the behavior is similar to that found at lower temperatures and larger couplings, albeit with a smaller gap. Little substructure is observed in the spectrum. These results appear quite similar to the experimental observations of Uchida *et al.* on $\text{La}_{2-x}\text{Sr}_x\text{CuO}_4$ (La214). Results for other high- T_c cuprates are very similar. Even the appearance of what Uchida *et al.*³ called an “isobestic” point (a point where conductivities for different densities cross) is reproduced in this figure. Finally, in the very-high-temperature regime [$T = 5t$ in Fig. 3(c)], the gap is completely filled at all densities, although a remnant of the upper Hubbard band can still be seen. The MIR band and Drude peak have merged into a single structure. In Fig. 3(d), we show $\sigma(\omega)$ in the region $1 < \omega < 5$ for $U/t = 8$ and $T = 1.25t$. For the case of $\langle n \rangle = 0.5$, $\sigma(\omega)$ can be accurately described by a $1/\omega^2$ law, as expected for a conventional Fermi liquid. In contrast, for $\langle n \rangle = 0.75$, $\sigma(\omega)$ has a much slower decay with ω and can be fitted by the form $(1/\omega^\alpha)$, with $\alpha = 1.3 \pm 0.2$. Both forms are included in this figure for comparison. As can be seen in Fig. 3(b) for seven

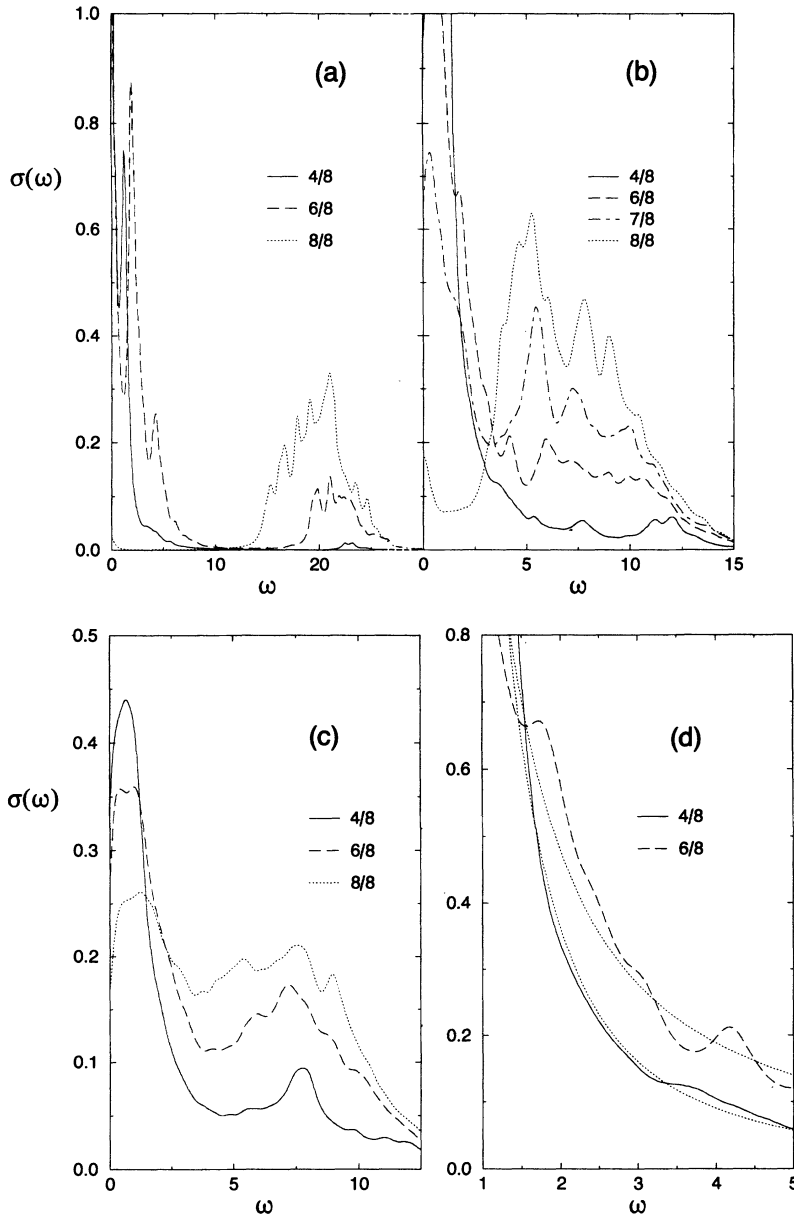


FIG. 3. (a) The real part of the optical conductivity as a function of frequency at different densities, for $U/t = 20$, $\epsilon = 0.33$, and $T = 0.3125t$; (b) as in (a) for $U/t = 8$ and $T = 1.25t$; (c) as in (b) for $T = 5t$; (d) $\sigma(\omega)$ at $U/t = 8$ and $T = 1.25t$ in the interval $1 < \omega < 5$, together with fits to $1/\omega^2$ ($\langle n \rangle = 0.5$) and $1/\omega^{1.3}$ ($\langle n \rangle = 0.25$), indicated by dotted lines. $\sigma(\omega)$ in arbitrary units, ω in units of the hopping parameter t .

electrons ($\langle n \rangle = 0.875$), $\sigma(\omega)$ has an even slower decay with ω for ω less than ≈ 3 . This anomalous frequency dependency of the conductivity has also been observed experimentally in La214.³ Moreover, a close correlation between the temperature dependence of ρ_{ab} and the frequency dependence of the scattering rate $1/\tau(\omega)$ (seen in the frequency dependence of the conductivity) was observed; $1/\tau(\omega) \sim \omega^{1.6}$ behavior in an overdoped sample of La214 was recently reported,¹⁴ which is quite reminiscent of our power-law fit.

In summary, we have reported a numerical exact-diagonalization calculation of the optical conductivity of the two-dimensional one-band Hubbard model. The dc resistivity shows linear behavior in T for $T > t$ and large U/t , which presumably is also valid in the lower-temperature range $J < T < t$. The ac conductivity was also calculated, and we have presented results at several temperatures. A MIR band is observed, together

with a Drude peak and charge excitations. The combination of the Drude and MIR oscillator strengths leads to a conductivity near half filling that decays somewhat more slowly than $1/\omega^2$ at energies smaller than the insulator gap.

Recently, we learned of an independent study by Jaklič and Prelovšek¹⁷ of the 2D t - J model at finite temperature using a different numerical method. Their results are qualitatively similar to our results for the Hubbard model.

Conversations with T. Barnes, M. Büttiker, E. Gagliano, A. Moreo, and H. Pastawski are gratefully acknowledged. J.R. was supported in part by the U. S. Department of Energy (DOE) Office of Scientific Computing, under the High Performance Computing and Com-

munications Program (HPCC), and in part by the DOE under Contract No. DE-AC05-84OR21400 managed by Martin Marietta Energy Systems, Inc., and under contract No. DE-FG05-87ER40376 with Vanderbilt University. E.D. is supported by the Office of Naval Research

under Grant No. ONR N00014-93-1-0495. The numerical calculations were done at the Supercomputer Computations Research Institute, Tallahassee, Florida and at the National Center for Supercomputing Applications, Urbana, Illinois.

¹B. Batlogg, *Phys. Today* **44**, 44 (1991); B. Batlogg, H. Takagi, H. L. Kao, and J. Kwo, in *Electronic Properties of High T_c Superconductors, The Normal and the Superconducting State*, edited by H. Kuzmany *et al.* (Springer-Verlag, Berlin, 1992).

²T. Ito, K. Takenaka, and S. Uchida, *Phys. Rev. Lett.* **70**, 3995 (1993).

³S. Uchida, T. Ido, H. Takagi, T. Arima, Y. Tokura, and S. Tajima, *Phys. Rev. B* **43**, 7942 (1991); D. B. Tanner and T. Timusk, in *Physical Properties of High-Temperature Superconductors III*, edited by Donald M. Ginsberg (World Scientific, Singapore, 1992), p. 363.

⁴E. Dagotto, *Rev. Mod. Phys.* (to be published).

⁵I. Sega and P. Prelovsek, *Phys. Rev. B* **42**, 892 (1990); A. Moreo and E. Dagotto, *ibid.* **42**, 4786 (1990); W. Stephan and P. Horsch, *ibid.* **42**, 8736 (1990); D. Poilblanc *et al.*, *ibid.* **47**, 14267 (1993).

⁶E. Dagotto, A. Moreo, F. Ortolani, D. Poilblanc, and J. Riera, *Phys. Rev. B* **45**, 10741 (1992).

⁷Monte Carlo techniques require analytical continuation from imaginary to real time to obtain dynamical observables; therefore, this procedure should also be compared to exact results obtained on finite clusters to test its accuracy.

⁸G. D. Mahan, *Many-Particle Physics* (Plenum, New York, 1991), p. 185.

⁹W. H. Press *et al.*, *Numerical Recipes* (Cambridge University Press, Cambridge, 1986).

¹⁰J. Oitmaa and D. D. Betts, *Can. J. Phys.* **56**, 897 (1978).

¹¹For details on the use of APBC (or more generally twisted BC) see J. A. Riera, *Phys. Rev. B* **43**, 3681 (1991).

¹²T. Giamarchi, *Phys. Rev. B* **44**, 2905 (1991).

¹³T. M. Rice and F. C. Zhang, *Phys. Rev. B* **39**, 815 (1989). See also N. Ohata and R. Kubo, *J. Phys. Soc. Jpn.* **28**, 1402 (1970).

¹⁴Deviations from linear T behavior in $\text{La}_{2-x}\text{Sr}_x\text{CuO}_4$ were reported in H. Takagi *et al.*, *Phys. Rev. Lett.* **70**, 3995 (1993). Similar results in overdoped samples of Y123 were reported in Ref. 2.

¹⁵Results for four electrons on the same cluster and five electrons on a $\sqrt{10} \times \sqrt{10}$ cluster show qualitatively similar behavior.

¹⁶Y. Imry, in *Directions in Condensed Matter Physics*, edited by G. Grinstein and G. Mazenko (World Scientific, Singapore, 1986).

¹⁷J. Jaklič and P. Prelovšek, University of Ljubljana (unpublished).